

Photocatalytic Degradation of Azo Dye (Methyl Red) In Water under Visible Light Using Ag-Ni/TiO₂ Sythesized by γ - Irradiation Method

Vo Thi Thu Nhu^{1,2}, Do QuangMinh¹, Nguyen Ngoc Duy³, Nguyen QuocHien^{3*}

¹Ho Chi Minh City University of Technology, 268 Ly ThuongKiet, District 10, Ho Chi Minh City, Vietnam

²University of Technical Education Ho Chi Minh City, 1 Vo Van Ngan Street, Thu Duc District, Ho Chi Minh City, Vietnam

³Research and Development Center for Radiation Technology, 202A Street 11, Linh Xuan Ward, Thu Duc District, Ho Chi Minh City, Vietnam

*Corresponding author.

E-mail address: hien7240238@yahoo.com (N.Q. Hien), Phone: 84 8 38975922, Fax: 84 8 38975921

Abstract— Commercial TiO₂ (P25) co-doped with bimetallic silver and nickel nanoparticles (Ag-Ni/TiO₂) was prepared by γ -irradiation method. The properties of Ag-Ni/TiO₂ were characterized by X-Ray diffraction (XRD), X-ray photoelectron spectroscopy (XPS), transmission electron microscopy (TEM), scanning electron microscopy (SEM), diffuse reflectance spectroscopy (DRS), energy dispersive X-ray spectroscopy techniques (EDX) and surface area measurement by Brunauer-Emmett-Teller (BET) method. The size of silver and nickel nanoparticles was determined by TEM to be of 1-2 nm. The photo-catalytic degradation of azo dye methyl red in the aqueous suspensions of TiO₂ and Ag-Ni/TiO₂ under visible light was carried out to evaluate the photo-catalytic activity. Results showed that Ag-Ni/TiO₂ was found to enhance photo-degradation efficiency of azo dye methyl red compared to commercial TiO₂. The results showed that Ag 3% (w/w) and Ni 1.5% (w/w) co-doped TiO₂ had the highest photoactivity among all studied samples under visible light. Thus, γ -irradiation method can be suitably applied to prepare photo-catalyst of Ag-Ni/TiO₂ with highly photocatalytic activity.

Keywords—TiO₂, silver, nickel, nanoparticles, photocatalytic, γ -irradiation.

I. INTRODUCTION

Photocatalytic reactions at the surface of titanium dioxide have been attracting much attention in view of their practical applications to environmental treatment [1]. The material TiO₂ is a well-known photocatalyst for its high efficiency, low cost, physical and chemical stability, widespread availability, and noncorrosive property [2]. NanoTiO₂ shows

relatively high reactivity and chemical stability under ultraviolet light (<387nm), whose energy exceeds the band gap of 3.2 eV in the anatase crystalline phase. The development of photocatalysts with high reactivity under visible light (> 400 nm) should allow the main part of the solar spectrum, even under poor illumination of interior lighting, to be used [3]. Several approaches for nanoTiO₂ modification have been reported [4]. These included dye sensitization, semiconductor coupling, impurity doping, use of coordination metal complexes, and metal deposition. A combination of two or more kinds of metals has been widely applied in various materials to enhance the performance and reliability of the materials. The incorporation of metals in the titanium dioxide crystal lattice may result in the formation of new energy levels between valence band and conduction band, inducing a shift of light absorption towards the visible light region. Possible limitations are photocorrosion and reduce charge recombination at metal sites [5].

The use of Ag and Ni for bimetallic catalyst has been reported as the effective method to improve the efficiency of various reactions [6, 7]. Ag-Ni/carbon nanotube for glucose oxidation [6]. Silver and nickel doped TiO₂ by sol-gel method applied against bacteria under UV and visible light irradiations [7].

Various methods for the synthesis of modified TiO₂ photocatalyst included precipitation [8], hydrothermal, solvothermal [9], chemical vapour deposition [10], and electrospinning [11], radiolysis [12]. Among several methods for modified nanopowder TiO₂, radiolysis method using γ -irradiation is advantageous because the experiment can be

carried out at very mild conditions, ambient pressure and room temperature with high reproducibility and it is the unique method [13, 14, 15]. In addition, Zhang et al. (2010) [16] also synthesized Ag-Ni alloy nanoparticles by radiolytic method. So, in this study, we reported the preparation of Ag and Ni-co-doped on TiO₂ (Ag-Ni/TiO₂) by γ -irradiation method and studied its photoactivity of degradation of methyl red in water. The properties of the catalysts were characterized by X-ray diffraction (XRD), diffuse reflectance spectroscopy (DRS), surface area measurement by Brunauer-Emmett-Teller (BET) method, transmission electron microscopy (TEM), scanning electron microscopy (SEM), energy dispersive X-ray spectroscopy techniques (EDX), X-ray photoelectron spectroscopy (XPS). The photocatalytic performance, reaction kinetic, and reusability of the catalysts were also investigated.

II. EXPERIMENTAL

2.1. Materials

Silver nitrate (AgNO₃) and nickel nitrate hexahydrate (Ni(NO₃)₂·6H₂O) were purchased from China used as dopant metal salts. Titanium dioxide, TiO₂ (Degussa P25) was from Germany used as the support and ethanol was from China. Methyl red from China was used as the model of organic pollutant for photocatalytic degradation study.

2.2. Sample preparation

A series of TiO₂ samples was prepared by codoping with silver and nickel in the range of 0.75–3% (w/w) by γ -irradiation method. 2 g TiO₂ and 10 ml ethanol were added into 90 ml distilled water and stirred. The required amount of AgNO₃ and NiNO₃ were then added to the TiO₂ suspension mixture with various mass ratios of Ag and Ni. The reduction of Ag⁺ and Ni²⁺ was carried out by γ -irradiation on a γ -⁶⁰Co source using gamma chamber GC – 5000, BRIT, India at the Nuclear Research Institute, Da Lat, Vietnam with dose rate of 2.5 kGy/h and absorbed dose range from 15.8 to 46.5 kGy measured by a dichromate dosimetry system [17] at room temperature and under atmospheric pressure. The TiO₂ doped with Ag and Ni photo-catalyst was separated by centrifugation, washed by distilled water and dried at 60°C. The detailed parameters of experiments were listed in Table 1.

2.3. Characterization of TiO₂ doped with Ag-Ni nanoparticles

The size of Ag and Ni nanoparticles doped on TiO₂ catalyst was characterized by TEM images on a JEM 1010, JEOL, Japan and XRD patterns were measured on D8 Advanced, Bruker, Germany using a Cu K α (λ = 0.15418 nm). The specific surface areas of samples were determined by nitrogen adsorption at 77K using Quantachrome 1994-2010 instrument of Germany using BET method. The solid UV-vis DRS was carried out using JASCO V550 model UV-vis spectrometer. XPS analyses were obtained with a ULVAC PHI instrument, equipped with Al K α X-ray source. The morphology and the elemental content of the catalyst were investigated with SEM (Hitachi SEM S-4800) coupled with a Genesis 4000 EDX spectrometer.

2.4. Photocatalytic degradation activity

0.025 g of photocatalyst was added to 50 mL methyl red (10⁻⁵ M). The solution with the catalyst was stirred in the dark for 1 hour for the solution to attain absorbed equilibrium. It was then irradiated using the 150 W halogen lamp (the visible light source) at a distance of 40 cm from the solution level and the temperature of the reactor was controlled at 30 ± 2°C. After period of time of 20, 40, 60, 80, 100 and 120 min, the aqueous suspension was filtered through centrifugation to remove catalyst particles. Each set of experiment was performed three times. MR concentration was estimated by colorimetric method using UV-vis spectrophotometer (Biochrom, Libra S32).

The photo-catalytic kinetic of methyl red degradation was described by the pseudo-first-order kinetic as follows:

$$v = -dC/dt = -kC \text{ (or } C = C_0 e^{-kt}) \quad (1)$$

Where v is the reaction rate, C is the concentration of MR dye at certain reaction time, C_0 is the initial concentration of MR, k is rate constant and t is reaction time.

After the integration of the equation (1), the model can be expressed by the following equation (2):

$$\ln\left(\frac{C_0}{C}\right) = kt \quad (2)$$

A plot of $\ln\left(\frac{C_0}{C}\right)$ with time will yield a linear plot with slope k .

III. RESULTS AND DISCUSSION

Table 1. Composition and absorbed dose for preparation of different Ag-Ni/TiO₂ samples

Sample name	Weight of precursor	V(H ₂ O): V (C ₂ H ₅ OH)	Dose (kGy)	Irradiation time (min)
Ag0.75-Ni1.5/TiO ₂	mAgNO ₃ = 0.0236 g mNi(NO ₃) ₂ .6H ₂ O = 0.1488 g	90 ml: 10 ml	23.3	1398
Ag1.5-Ni0.75/TiO ₂	mAgNO ₃ = 0.0472 g mNi(NO ₃) ₂ .6H ₂ O = 0.0744 g	90 ml: 10 ml	15.8	948
Ag1.5-Ni1.5/TiO ₂	mAgNO ₃ = 0.0472 g mNi(NO ₃) ₂ .6H ₂ O = 0.1488 g	90 ml: 10 ml	26.0	1560
Ag1.5-Ni3.0/TiO ₂	mAgNO ₃ = 0.0472 g mNi(NO ₃) ₂ .6H ₂ O = 0.2976 g	90 ml: 10 ml	46.5	2790
Ag3.0-Ni1.5/TiO ₂	mAgNO ₃ = 0.0944 g mNi(NO ₃) ₂ .6H ₂ O = 0.1488 g	90 ml: 10 ml	31.6	1896

The absorbed doses presented in Table 1 were calculated based on the dose of ~1.67 kGy for reduction of 1 mM Ag⁺[18], but in excess for 20% .

3.1. Characterization of catalysts

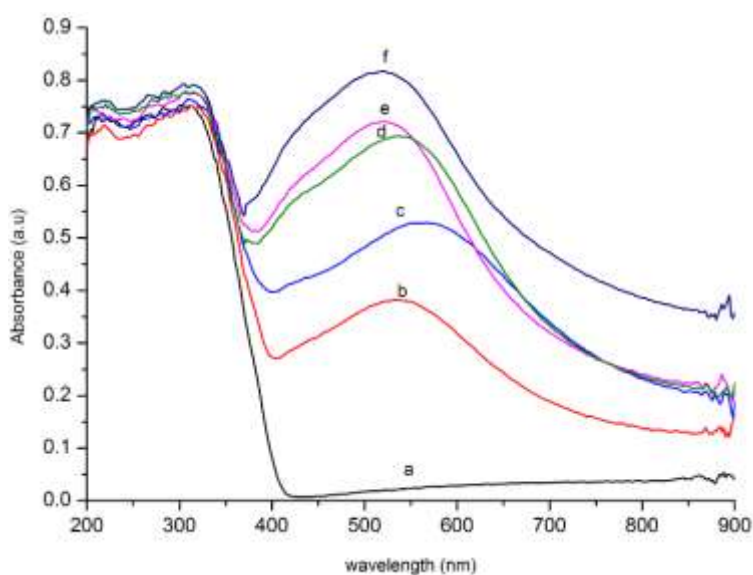


Fig.1: UV-vis Diffuse reflectance spectra (DRS) of pure TiO₂ and modified TiO₂: (a) Pure TiO₂; (b) Ag0.75-Ni1.5/TiO₂; (c) Ag1.5-Ni0.75/TiO₂; (d) Ag1.5-Ni3.0/TiO₂; (e) Ag1.5-Ni1.5/TiO₂; (f) Ag3.0-Ni1.5/TiO₂

The UV-visible spectral of the pure TiO₂ and modified TiO₂ by Ag and Ni in the range of 200 to 900 nm were shown in Fig. 1. It was found that the absorbance of Ag-Ni/TiO₂ in the visible region was always higher than that for pure TiO₂. The absorption peak of Ag-Ni/TiO₂ shifted towards the

visible region. The visible-light photo absorption of Ag3.0-Ni1.5/TiO₂ was the highest among studied samples. The absorption of the modified TiO₂ samples in the range of 510–570 nm was probably due to Ag and Ni nanoparticles which absorbed in this spectral range.

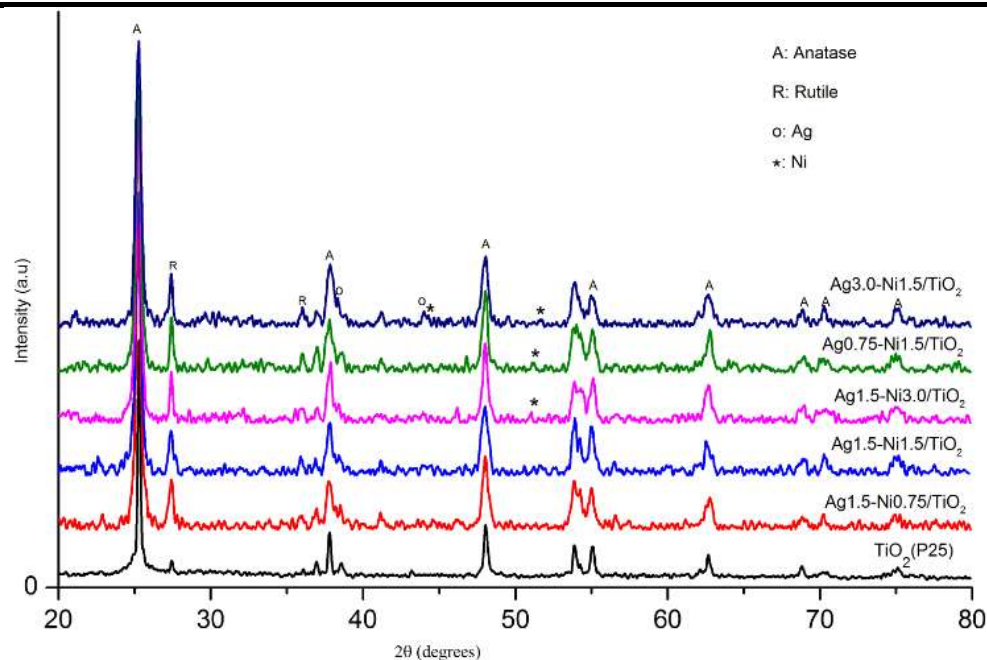


Fig. 2. XRD patterns of TiO_2 (P25) and Ag-Ni/TiO_2 with various content of Ag and Ni.

Fig. 2 showed the typical XRD patterns of the pure TiO_2 (P25), and TiO_2 doped with various content of Ag and Ni. It is clearly from Fig. 2 that original TiO_2 powder exhibits typical pattern that indicate for the phases of anatase and rutile. The XRD pattern of Ag3.0-Ni1.5/TiO_2 consisted of peaks at 25.2° ; 37.6° ; 48.0° ; 53.9° ; 55.1° ; 62.4° ; 68.7° ; 70.2° and 75.1° correspond to the crystal planes [101], [004], [200], [105], [211], [204], [220], [220] and [215] respectively; this is indicate for phase anatase of TiO_2 ,

whereas rutile crystallites structure has peaks at 27.4° and 36.1° correspond to the crystal planes [110] and [101]. Peaks at 2θ values of 38.1° , 44.1° that reflect the cubic Ag phase which can be attributed to the crystal planes of metallic silver [111] and [200], respectively. Peaks at 2θ values of 44.5° and 51.7° that indicated for crystal planes of metallic nickel [111] and [200]. All peaks for Ag and Ni were weak because of the low content of silver and nickel.

Table.2: θ values of [101] plane and [200] plane of TiO_2 after doping by Ag and Ni with different content

Ag content, % (w/w)	0.0 (TiO_2)	0.75	1.5	1.5	1.5	3.0
Ni content, % (w/w)	0.0 (TiO_2)	1.5	0.75	1.5	3.0	1.5
2θ [101] plane	25.5	25.37	25.34	25.21	25.42	25.22
2θ [200] plane	48.29	48.16	48.13	47.98	48.17	48.02

In addition, from the results of XRD in Table 2, it can be seen that the position of TiO_2 plane [101] and [200] change the angle by doping with Ag and Ni. According to Bragg's law: $n\lambda = 2d\sin\theta$ [19], can be drawn that the lesser is the value of $\sin\theta$, the larger is the d spacing. Opposite, the larger is the value of $\sin\theta$, the lesser is the d spacing. So we can conclude that the value of d spacing change with Ag and Ni doping, which implies that nickel and silver ions diffused into the lattice of TiO_2 .

Table.3: Sample, BET surface area of pure TiO_2 and Ag-Ni doped TiO_2 samples

Sample	BET surface area (m^2/g)
TiO_2	69.417
$\text{Ag0.75-Ni1.5/TiO}_2$	53.083
$\text{Ag1.5-Ni0.75/TiO}_2$	55.991
Ag1.5-Ni1.5/TiO_2	56.200
Ag1.5-Ni3.0/TiO_2	53.747
Ag3.0-Ni1.5/TiO_2	51.800

The surface areas of pure TiO_2 and Ag-Ni/ TiO_2 with various content of Ag and Ni were determined by the nitrogen gas adsorption method and shown in Table 3. The results in Table 3 showed that the surface area of Ag-Ni/ TiO_2 samples decreased compared to that of TiO_2 .

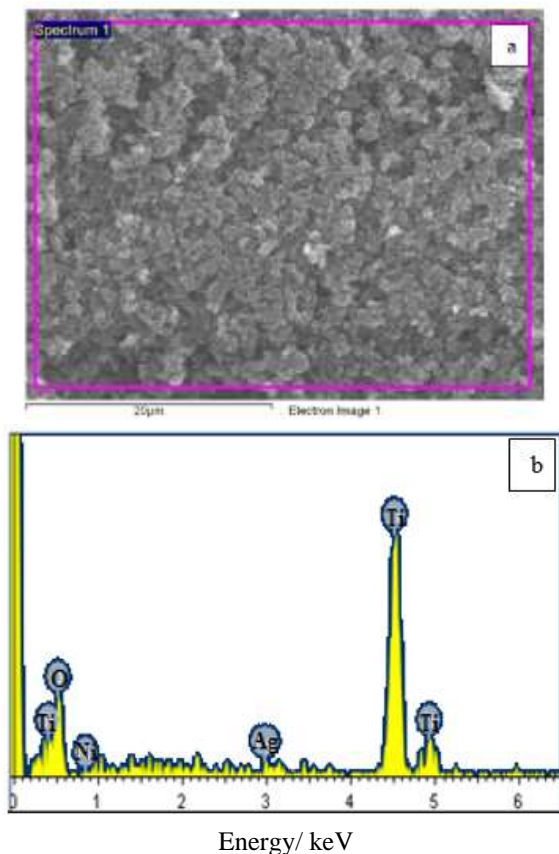


Fig. 3: SEM image (a) and EDX diagram (b) of Ag_{3.0}-Ni_{1.5}/TiO₂ catalyst

The SEM micrograph and EDX spectrum of Ag_{3.0}-Ni_{1.5}/TiO₂ catalyst were shown in Fig. 3. The SEM micrograph showed catalyst particles with spherical morphology. The composition of the Ag_{3.0}-Ni_{1.5}/TiO₂ catalyst was determined by EDX analysis. The EDX spectrum was recorded in the binding energy region of 0 - 6 eV which was shown in Fig. 3b. The existence of Ag and Ni atoms on the TiO₂ was confirmed.

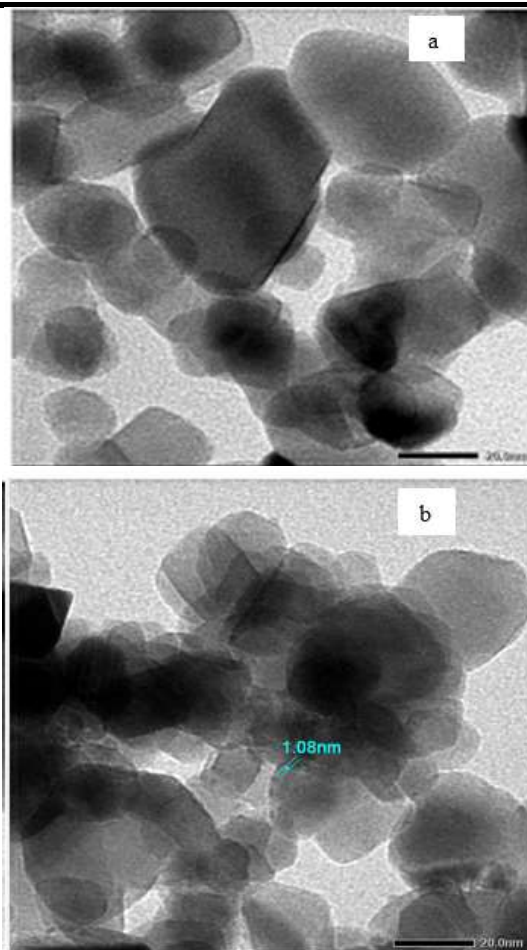


Fig. 4: TEM images of TiO₂ (P25) (a) and Ag_{3.0}-Ni_{1.5}/TiO₂ (b) photocatalyst

The morphology and metal distribution of the catalysts were then examined by TEM images. Fig. 4 showed the TEM images of TiO₂ (P25) and Ag_{3.0}-Ni_{1.5}/TiO₂. TEM image of TiO₂ in Fig. 4a indicated that the TiO₂ particles have not agglomerated. The average size of particles of TiO₂ was estimated to be 10 - 40 nm. TEM image of Ag_{3.0}-Ni_{1.5}/TiO₂ in Fig. 4b indicated that Ag and Ni nanoparticles with size of about 1-2 nm were dispersed on the surface of TiO₂. The size of TiO₂ particles was almost unchanged for TiO₂ and Ag_{3.0}-Ni_{1.5}/TiO₂ sample.

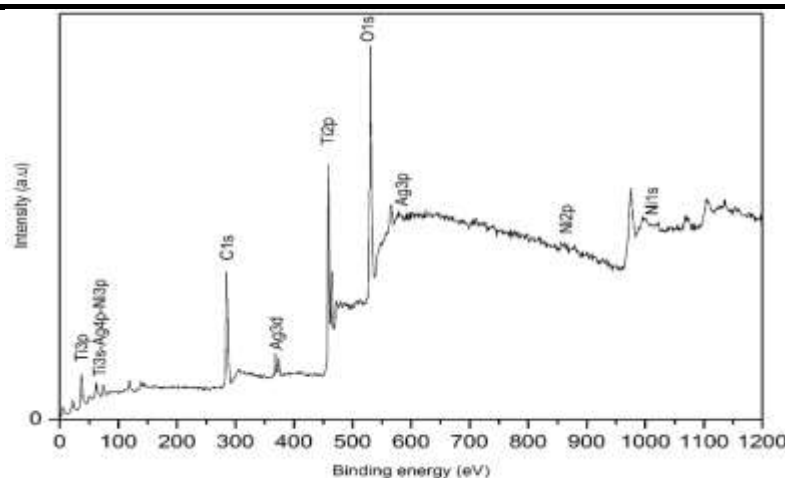


Fig. 5: XPS full survey of Ag_{3.0}-Ni_{1.5}/TiO₂

XPS analysis of silver and nickel co-doped TiO₂ sample (Ag_{3.0}-Ni_{1.5}/TiO₂) was performed and shown in Fig. 5. The XPS full spectrum showed the presence of different elements on the surface of the catalyst. XPS analysis of Ag_{3.0}-Ti_{1.5}/TiO₂ sample detected peaks of Ti, O, C, Ni and Ag. The presence of C was attributed to carbon contamination existed on the sample rack.

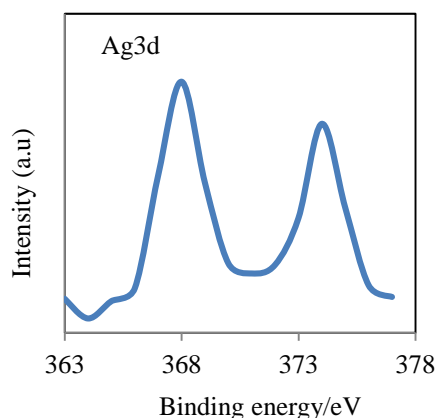


Fig. 6: XPS survey for Ag_{3d}

Fig. 6 showed that the catalyst exhibited their Ag_{3d} level two peaks (at around 368 and 374 eV), which indicated for the Ag 3d_{5/2} and 3d_{3/2}. The binding energy of peak Ag 3d_{5/2} maximum at 368.1 eV was close to the value reported for metallic Ag(0) [12].

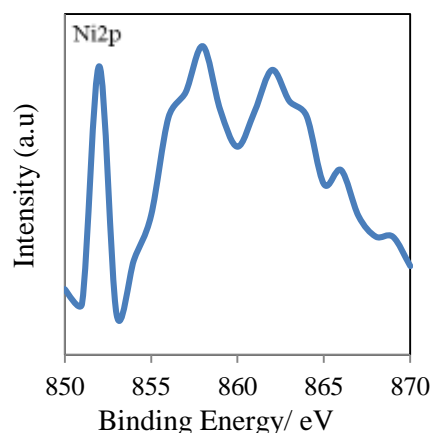


Fig. 7: XPS survey for Ni_{2p}

The Ni 2p_{3/2} regions of the Ag_{3.0}-Ti_{1.5}/TiO₂ catalyst showed several peaks in the range of 850–870 eV (Fig. 7). The first peak at 852.1 eV resulted for metallic nickel Ni(0) [20]. The second peak at 858.1 eV was attributed to Ni²⁺ ions within the composite oxide structure [21], whereas the peak at 862 eV was assigned to its corresponding shake-up satellite lines. The detection of metallic nickel Ni(0) clearly indicated a reduction of the ion Ni²⁺ on the surface of the catalyst.

3.2. Photocatalytic degradation of methyl red

3.2.1. Effect of dopant content

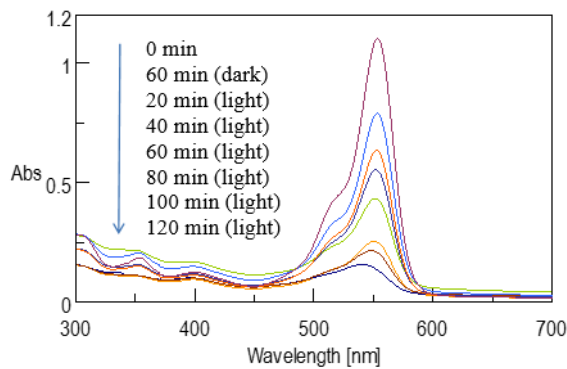


Fig. 8: Absorption spectra of MR at different time interval degraded by the Ag1.0-Ni0.75/TiO₂ catalyst under visible light.

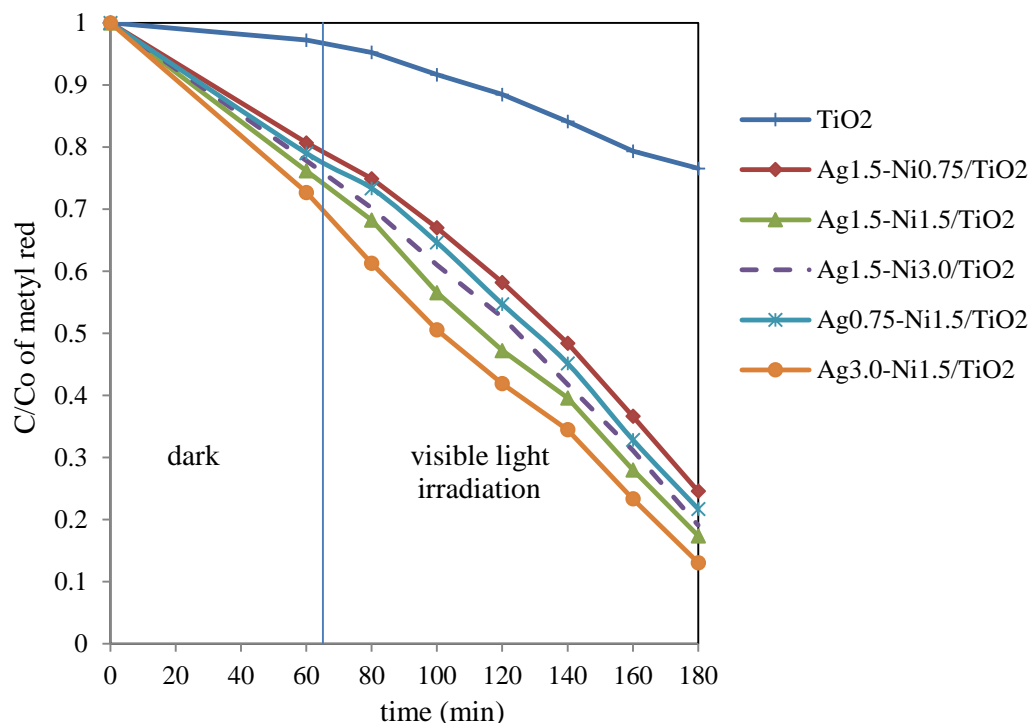


Fig.9: Degradation of MR under visible irradiation by TiO₂ and Ag-Ni/TiO₂ with different dopant (Ag and Ni) content. The initial concentration of MR: $1 \times 10^{-5} M$, amount of catalyst: 0.5 g/L.

Photocatalytic degradation of MR by pure TiO₂ and Ag and Ni co-doped on TiO₂ catalysts with various dopant concentrations under visible light was presented in Fig. 9. The effect of dopant on the percentage of methyl red degradation was studied with different amount of Ag and Ni varying from 0.75 to 3.0 % (w/w), with MR solution concentration of $10^{-5} M$ and amount of catalyst of 0.5 g/L. All the Ag-Ni/TiO₂ samples showed higher photocatalytic activity than that of commercial TiO₂ (Degussa P25) under visible light irradiation. Thus modified TiO₂ by Ag and Ni

Fig.8 showed the absorption spectra of MR before and after irradiating under the visible light for different time interval using Ag1.0-Ni0.75/TiO₂ as a photocatalyst. The intensity of the peak was found to decrease with increasing irradiation time during photocatalytic degradation of MR. It proves that the concentration of MR decreased with increasing degradation time.

nanoparticles resulted in higher photocatalytic activity. Among catalysts, the sample containing 3% Ag and 1.5% Ni (w/w) performed the highest photodegradation efficiency.

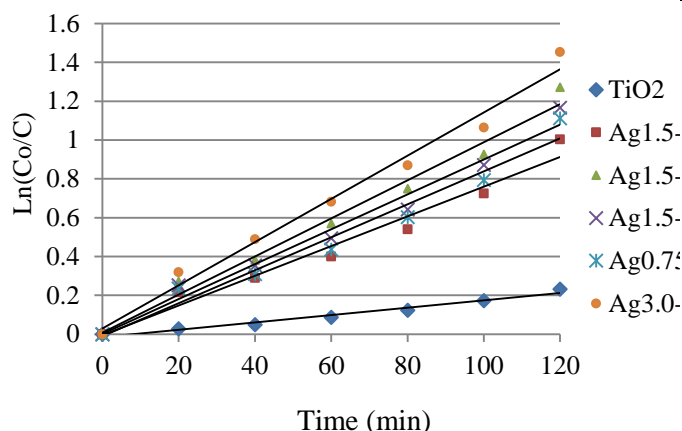


Fig.10: $\ln(C_0/C)$ versus irradiation time for MR under visible light by TiO_2 and Ag-Ni/ TiO_2 catalysts with initial concentration of MR: 10^{-5}M , amount of catalyst: 0.5 g/L.

As a result, the photodegradation kinetics fitted well with the pseudo first-order model that showed in Fig. 10. Degradation rate constants calculated from the results in Fig. 10 were of 0.0019; 0.0077; 0.0085; 0.009; 0.0098 and 0.0111 min^{-1} for TiO_2 , Ag1.5-Ni0.75/ TiO_2 , Ag0.75-Ni1.5/ TiO_2 , Ag1.5-Ni3.0/ TiO_2 , Ag1.5-Ni1.5/ TiO_2 and Ag3.0-Ni1.5/ TiO_2 , respectively. The sample with 3 % Ag (w/w) and 1.5 % Ni (w/w) doped on TiO_2 exhibited the highest rate constant.

3.2.2. Effect of pH

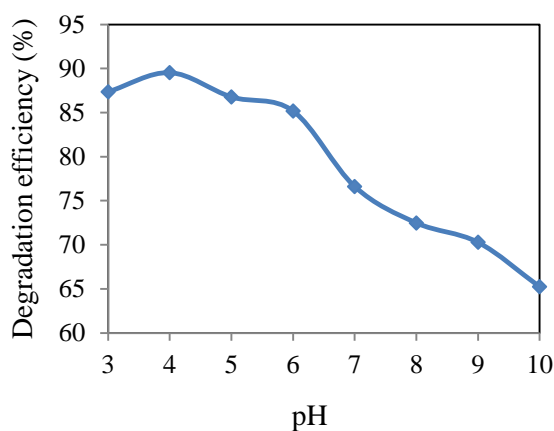


Fig. 11: The effect of pH on photodegradation of MR (amount of catalyst: 2.0 g/L; irradiation time: 60 min; MB initial concentration: 10^{-5}M ;

The pH of a dye solution is an important parameter that affects the rate of degradation. The effect of pH on photocatalytic degradation of MR was investigated with content of catalyst (Ag3.0-Ni1.5/ TiO_2) of 0.5 g/L, concentration of

MR of 10^{-5}M , irradiation time of 60 min and the range of pH from 3 to 10. PH was adjusted by 1N HNO_3 and 1N NaOH . Fig. 11 showed the degradation efficiency of MR at different pH values. The results clearly showed that photocatalytic degradation of the MR dye increased to pH 4 and then decreased significantly to pH 10. The maximum MR degradation of 89.18% was observed at pH 4. This may be explained that the higher degradation extent of MR occurred in acidic medium rather than alkaline. Hence, at acidic pH values, the particle surfaces of catalysts are positively charged and at basic pH values, they are negatively charged [22]. In acidic environment, the adsorption of anionic dye molecules on the surface of the catalyst particle increased. Moreover, in acidic pH the photo excited electrons in the photocatalyst could be fast abstracted from the surface by the numerous protons of the medium [23].

3.2.3. Effect of catalytic content

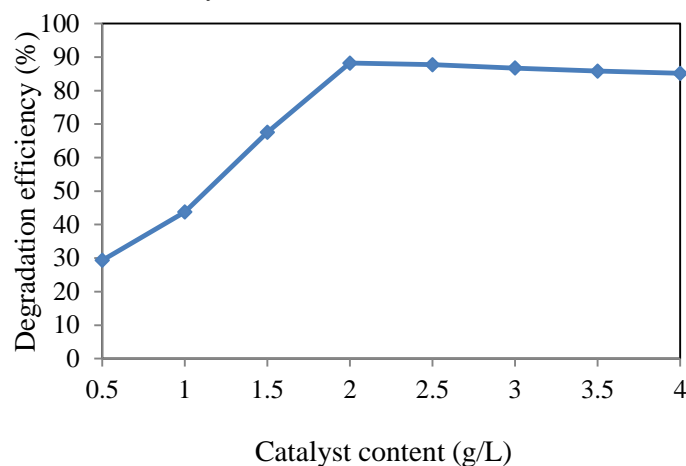


Fig. 12: Degradation at different content of Ag3.0-Ni1.5/ TiO_2 catalyst (MR initial concentration: 10^{-5}M ; pH: 4; irradiation time: 60 min).

The effect of catalyst content (Ag3.0-Ni1.5/ TiO_2) on the degradation efficiency of MR was investigated with different catalytic content varying from 0.5 to 4.0 g/L, at dye solution concentration: 10^{-5}M for 60 min and pH at 4. The results were shown in Fig.12. The degradation efficiency significantly increased up to 2 g/L of catalytic content. When catalytic content was more than 2.0 g/L, the degradation efficiency of dye was found to be almost unchanged. Therefore, an optimum catalytic dose of 2 g/L was selected for further experiment.

3.2.4. Effect of irradiation time

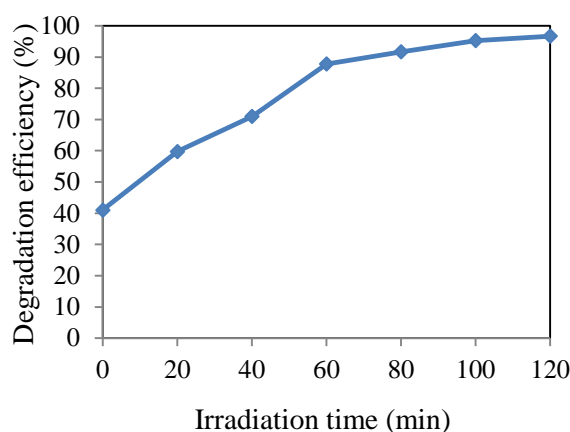


Fig. 13: The effect of irradiation time on photodegradation of MR (catalyst content: 2.0 g/L; pH: 4; MR initial concentration: $10^{-5}M$).

In order to study the effect of irradiation duration on the degradation efficiency on MR, the experiments were carried out with Ag_{3.0}-Ni_{1.5}/TiO₂ catalyst amount of 2.0 g/L; pH of dye solution at 4, initial concentration of MR of $10^{-5}M$ and irradiation time of the dye solution in the range from 0 to 120 min. The results in Fig. 13 indicated that the degradation percentage increased with the increase of irradiation time. At the irradiation time of 120 min, the percent degradation of MR achieved 96.7%.

3.2.5. Reuse of the photocatalyst

To determine the ability of reuse of Ag-Ni/TiO₂ as a photocatalytic, reuse experiment of the photocatalytic activity of Ag_{3.0}-Ni_{1.5}/TiO₂ catalyst was performed. After degradation of MR, the photocatalyst was then washed with distilled water and dried. Then the catalyst was reused for degradation of MR solution. The results in Fig. 14 showed that after four times of reuse, the catalyst was still active with a slight decrease in the degradation efficiency from 96.7% (first cycle) to 89.1% (fifth cycle). Hence, it can be confirmed that the photocatalytic activity of Ag-Ni/TiO₂ catalyst was almost stable during degradation of MR.

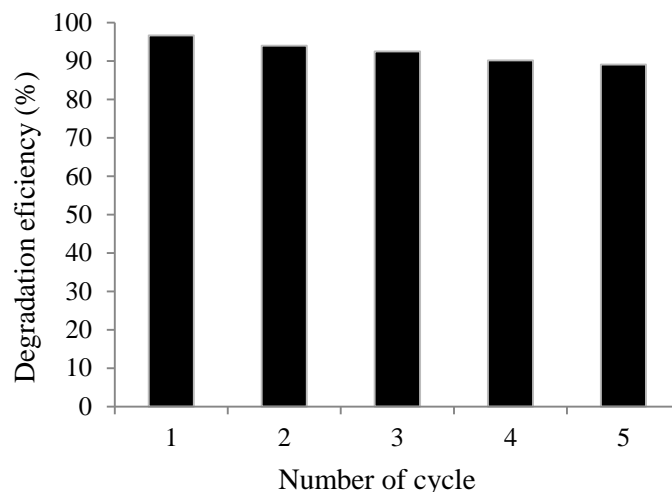


Fig. 14: Regeneration of Ag_{3.0}-Ni_{1.5}/TiO₂ photocatalyst on degradation of MR (amount of catalyst: 2.0 g/L; pH: 4; MR initial concentration: $10^{-5}M$; irradiation time: 120 min).

IV. CONCLUSION

Co-doping Ag and Ni nanoparticles on TiO₂ with different amount of Ag and Ni was carried out by γ -irradiation method. The presence of Ag and Ni in the crystal lattice of TiO₂ was confirmed. The size of Ag and Ni nanoparticles on the surface of TiO₂ was of 1-2 nm. Ag-Ni/TiO₂ photocatalysts displayed higher photocatalytic activity for pure TiO₂. Among all synthesized catalysts, the TiO₂ modified with 3.0% Ag (w/w) and 1.5% Ni (w/w) exhibited the highest photocatalytic activity under visible light. In addition, the Ag_{3.0}-Ni_{1.5}/TiO₂ photocatalyst can be reused many times with almost unchanged photocatalytic activity. Thus, Co-doping TiO₂ with silver and nickel by γ -irradiation can be suitably used as a photocatalyst for degradation of organic pollutants in water.

REFERENCES

- [1] Fujishima X., Zhang C. R. 2006. "Titanium dioxide photocatalysis: Present situation and future approaches". *Chimie* 9, 750–760.
- [2] Di Paola A., Cufalo G., Addamo M. et al. 2008. "Photocatalytic activity of nanocrystalline TiO₂ (brookite, rutile and brookite-based) powders prepared by thermohydrolysis of TiCl₄ in aqueous chloride solutions". *Colloid Surface A* 317 (1–3), 366–376.
- [3] Seery M. K., George R., Floris P., Pillai, S.C. 2007. "Silver doped titanium dioxide nanomaterials for enhanced visible light photocatalysis". *J. Photochem. Photobiol. A: Chem.* 189 (2–3), 258–263.

- [4] Hariprasad N., Anju S. G., Yesodharan E. P., Suguna Y. 2013. "Sunlight induced removal of Rhodamine B from water through semiconductor photocatalysis: effects of adsorption, reaction conditions and additives". *Res. J. Mater. Sci.* 1, 9–17.
- [5] Demeestre K., Dewulf J., Ohno T., Salgado P. H., Langenhove H.V. 2005. "Visible light mediated photocatalytic degradation of gaseous trichloroethylene and dimethyl sulfide on modified titanium dioxide". *Appl. Catal. B: Environ.* 61 (1–2), 140–149.
- [6] Ouyang R., Zhang W., Zhou S., Yang Y., Ji Y., Feng K., Liang X., Xiao M., Miao Y. 2016. "Single walled carbon nanotube sandwiched Ni-Ag hybrid nanoparticle layers for the extraordinary electrocatalysis toward glucose oxidation". *Electrochimic. Acta* 188, 197–209.
- [7] Ubongchonlakate K., Sikong L., Tontai T., Saito F. 2010. "P. aeruginosa inactivation with silver and nickel doped TiO₂ films coated on glass fiber roving". *Adv. Mater. Res.* 150-151, 1726–1731.
- [8] Dvoranova D., Brezova V., Mazur M., Malathi M.A. 2002. "Investigations of metal-doped titanium dioxide photocatalysts". *Appl. Catal. B: Environ.* 37, 91–105.
- [9] Zhu J., Deng Z., Chen F. et al. 2006. "Hydrothermal doping method for preparation of Cr³⁺-TiO₂ photocatalysts with concentration gradient distribution of Cr³⁺". *Appl. Catal. B: Environ.* 62 (3–4), 329–335.
- [10] Wu G., Nishikawa T., Ohtani B., Chen A. 2007. "Synthesis and characterization of carbon-doped TiO₂ nanostructures with enhanced visible light response". *Chem. Mater.* 19 (18), 4530–4537.
- [11] Patil K.R., Sathaye S.D., Kholam Y.B., Deshpande S.B., Pawaskar N.R., Mandale A.B. 2003. "Preparation of TiO₂ thin films by modified spin-coating method using an aqueous precursor". *Mater. Lett.* 57 (12), 1775–1780.
- [12] Grabowska E., Zaleska A., Sorgues S., Kunst M., Etcheberry A., Colbeau-Justin C., Remita H. 2013. "Modification of titanium(IV) dioxide with small silver nanoparticles: Application in photocatalysis". *J. Phys. Chem. C* 117 (4), 1955–1962.
- [13] Khatouri J., Mostafavi M., Amblard M., Belloni J. 2016. "Radiation induced copper aggregates and oligomer". *Chem. Phys. Lett.* 191, 351–356.
- [14] Belloni J. 1996. "Metal nanocolloids". *Curr. Opin. Colloid Interface Sci.* 1, 184–196.
- [15] Hayes D., Micic O. I., Nenadovitt M. T., Swayambunathan V., Meisel, D. 1989. "Radiolytic production and properties of ultrasmall cadmium sulfide particles". *J. Phys. Chem.* 93, 4603–4608.
- [16] Zhang Z., Nenoff T. M., Leung K., Ferreira S. R., Huang J. Y., Berry D.Y., Provencio P. P., Stumpf R. 2010. "Room temperature synthesis of Ag-Ni and Pd-Ni alloy nanoparticles". *J. Phys. Chem: C* 114, 14304–14318.
- [17] ASTM International, 2004. "Standard practice for use of a dichromate dosimetry system, ISO/ASTM 51401:2003(E)". Standards on dosimetry for radiation processing, pp. 69–74.
- [18] Remita S., Fontaine P., Rochas C., Muller F., Goldman M. 2005. "Radiation induced synthesis of silver nanoshells formed onto organic micelles". *Eur. Phys. J. D* 34, 231–233.
- [19] Suwarnkar M. B., Dhabbe R.S., Kadam A. N., Garadkar K.M. 2014. "Enhanced photocatalytic activity of Ag doped TiO₂ nanoparticles synthesized by a microwave assisted method". *Ceram. Int.* 40, 5489–5496.
- [20] Galtayries A., Grimblot J. 1999. "Formation and electronic properties of oxide and sulphide films of Co, Ni and Mo studied by XPS". *J. Electron Spectrosc. Relat. Phenom.* 98–99, 267–275.
- [21] Wang H., Xiang X., Li F., Evans D. G, Duan X. 2009. "Investigation of the structure and surface characteristics of Cu-Ni-M(III) mixed oxides (M = Al, Cr and In) prepared from layered double hydroxide precursors", *Appl. Surf. Sci.* 255, 6945–6952.
- [22] Guillard H., Lachheb A., Houas M., Ksibi C., Elaloui E., Herrmann J.M. 2003. "Influence of chemical structure of dyes, of pH and of inorganic salts on their photocatalytic degradation by TiO₂ comparison of the efficiency of powder and supported TiO₂". *J. Photochem. Photobiol. A: Chem.* 158, 27–36.
- [23] Lydia, I.S., Merlin, J.P., Dhayabaran, V.V., Radhika, N. 2012. Photodegradation of methyl red using Ag-doped Fe₃O₄ nanoparticles. *Int. J. Chem. Environ. Eng.* 3(4), 209–216.